THE ELECTROCHEMICAL REDUCTION OF OXYGEN ON COBALT-CEMENTED TUNGSTEN CARBIDE

ASHOK K. VIJH, R. JACQUES and G. BÉLANGER

Institut de recherche d'hydro-Québec, Case Postale 1000, 1800 Montée Sainte-Julie, Varennes, Qué., JOL 2 PO (Canada)

(Received August 22, 1981)

Summary

The electrochemical reduction of oxygen has been examined on cobalt-cemented tungsten carbide and on WC electrodes in alkaline solutions. The kinetics have been studied on a rotating disk electrode and the variation of reaction rate with electrode potential, temperature, oxygen concentration, solution pH and the rotation has been investigated. Rather high "Tafel slopes", low apparent heats of activation, negligible pH effect, unity reaction order with respect to oxygen and only a slight dependence on the rate of rotation (and that only at higher current densities) are the principal kinetic features. A chemical rate-determining-step (r.d.s.) has been concluded to be consistent with these data.

A comparison of the electroactivity of these electrodes for O_2 and H_2O_2 reduction shows that, at a given electrode potential, reduction of H_2O_2 proceeds at much higher rates than the reduction of O_2.

Introduction

The electro-reduction of oxygen is a central reaction in electrochemistry in that it is intimately connected with two fundamental problems, namely, the electrochemical stability of materials and the electrocatalysis at surfaces. Thus the importance of this reaction is clear in corrosion, fuel cells and metal–air batteries, etc.

We have previously examined the activity of metal carbides, especially those "cemented" by cobalt, for the anodic oxidation of a number of molecules such as hydrazine [1]. Here we examine the electrochemical activity of these cemented carbides towards the oxygen reduction reaction (o.d.r.).

Experimental

The electrochemical cell, electrodes, solutions, and instruments used in this study have been described recently [1]. It remains to give here the details on the rotating disk assembly utilized in the present work.

0378-7753/83/0000-0000/$03.00

The rotating disk apparatus used was from ESB Research Scientific Instrument Division and was model Depack XLR-2 combined with XLR-S10 readout system for the measurement of RPM (rotations per minute). The system allows the speed control through a digital panel meter for convenient and accurate readout of RPM or square root of RPM.

The disk electrode was made from a WC (or Co–WC) cylinder press-fitted into a hot rod of Kel-F. The geometric surface area of the electrode was 0.3147 cm^2. The electrode was polished mechanically on a rotating plate equipped with a silk cloth wetted with kerosene to support the diamond paste of 0.3 μm. After polishing the electrode was washed in ethanol in an ultrasonic bath and dried under vacuum. The electrode was subsequently washed with triple distilled water, just before placing it in the cell for electrochemical measurements.

The reference electrode was a home-made Hg/HgO (1M KOH) whose potential was verified to be 0.926 V *vs.* the hydrogen electrode in the same solution. All the potential scales quoted in this paper refer to a reversible hydrogen electrode (RHE) in the same solution, unless stated otherwise. The counter electrode was WC and was separated from the working compartment by means of a solution-sealed stopcock. No pre-electrolysis was conducted since it tends to add, rather than eliminate, impurities in the solutions of extreme pH values, especially with non-noble metal electrodes; platinum electrodes cannot, of course, be employed for the pre-electrolysis since they would introduce minute traces of the catalytic metal into the solutions.

As detailed in the previous study [1], the cobalt-cemented working electrodes were claimed by the manufacturer (Canadian General Electric, Carboloy Division) to contain 8.5% of Co. An X-ray fluorescence analysis of the polished electrode surface showed the cobalt content to be around 8%, both before and after the electrochemical polarization of the electrode; analyses performed on different parts of the sample showed that the Co content was uniform throughout the electrode.

Results

In this section, we first present the detailed results on the kinetics of o.d.r. on cobalt-cemented WC and, subsequently, compare their salient features with those of the o.d.r. on WC. The cobalt-cemented WC will here be designated as Co–WC. In the absence of oxygen, the Co–WC electrodes show anodic dissolution currents at potentials more anodic than about 0.7 V (RHE); with oxygen bubbling in the solution, such anodic dissolution currents disappear. The electrode is stable after the first "conditioning" potentiostatic curve, especially in the potential region 0 - 0.7 V (RHE) in the presence of oxygen. The results presented below refer to these stable electrodes.

(i) Current–potential relationships

The point-by-point potentiostatic current–potential curves in the descending direction (0.7 → 0.0 V) of potentials pertaining to the reduction

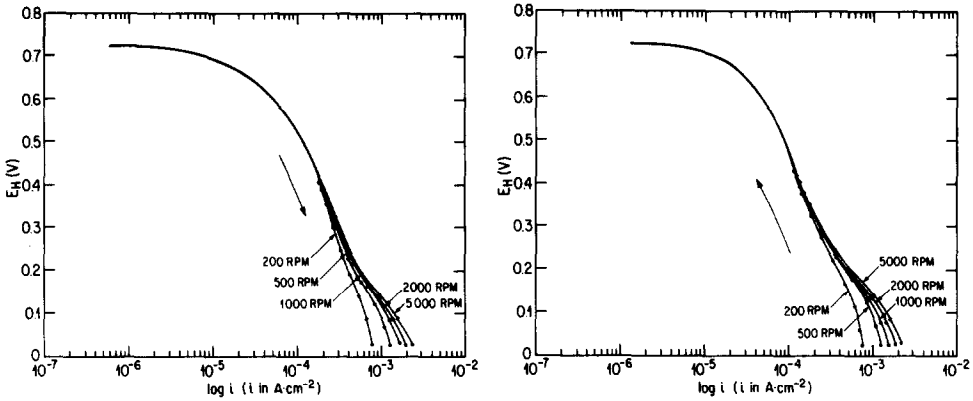

Fig. 1. A point-by-point potentiostatic potential–log [current] relationship for the oxygen dissolution reaction (o.d.r.) on Co–WC in 1M KOH solutions at various rotation rates of the disk electrode; temperature is 25 °C. The curves have been obtained in the descending direction of electrode potentials (w.r.t. hydrogen electrode in the same solution), as shown by the direction of the arrow.

Fig. 2. As in Fig. 1 but now the plots refer to the ascending direction of potentials, as indicated by the arrow.

of oxygen on Co–WC are presented in Fig. 1, as a function of the electrode rotation rate; the corresponding curves in the ascending direction (0.0 V → 0.7 V) of electrode potentials are shown in Fig. 2. It is clear that the electrode rotation has an effect on the reaction rate only at very high overpotentials for the reduction of O_2 since this effect manifests itself in the range *ca.* 0 - 0.3 V (RHE). No clear-cut Tafel line is observed although a region of high slope is indicated in current–potential curves.

The curves in the ascending and the descending directions of potentials are presented separately in order to avoid unnecessary clutter in the graphs; owing to the hysteresis effects, the curves in the two directions are slightly dissimilar.

(ii) The effect of temperature on the reaction rate

When the rate of oxygen reduction is examined potentiostatically at different temperatures (Figs. 3 and 4), a linear Tafel region of a slope $\approx RT/F$ is obtained only at 0 °C; this linear region disappears at higher temperatures, perhaps owing to the difficulties arising from the lowered stability of the electrode surface at higher temperatures. As regards the other features, regions of high slopes (sometimes called the "transition" regions in studies on anodic passivation) are observed, as in Figs. 1 and 2. The values of the apparent heats of activation (Figs. 5, 6) derived from Figs. 3 and 4, respectively, are generally lower than those indicative of a clear-cut activation control. In general, around the highest overpotential for the oxygen reduction reaction studied here, *e.g.*, 0.05 V (RHE), the apparent heat of activaction, ΔH^*, value is lower than 5 kcal, thus indicating a diffusion control;

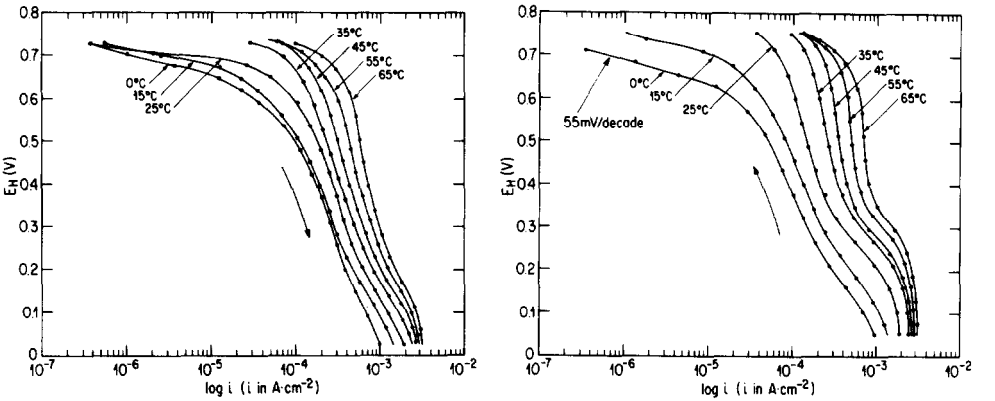

Fig. 3. Potentiostatic potential–log [current] relationships (as in Figs. 1 and 2) on Co–WC in 1M KOH solutions at the shown temperatures, in the descending direction of electrode potentials (see arrow). The rotation rate of the disk electrode is 2000 r.p.m.

Fig. 4. As in Fig. 3 but now in the ascending direction of potentials (see the arrow).

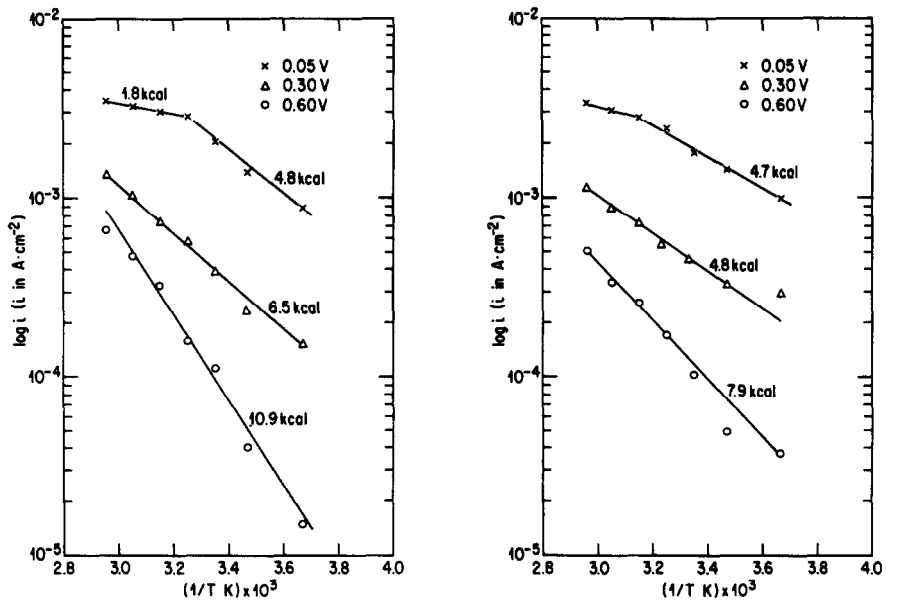

Fig. 5. Plots of reaction rates (*i.e.*, current densities) at the shown electrode potentials (as read from Fig. 3) against $1/T$, where T is the temperature in K. These plots are for the descending direction of electrode potentials (*i.e.*, Fig. 3); the values of the apparent heat of activation, ΔH^*, as derived from these plots are also indicated.

Fig. 6. As in Fig. 5 but now for the ascending direction of electrode potentials; the primary data for these plots are from Fig. 4.

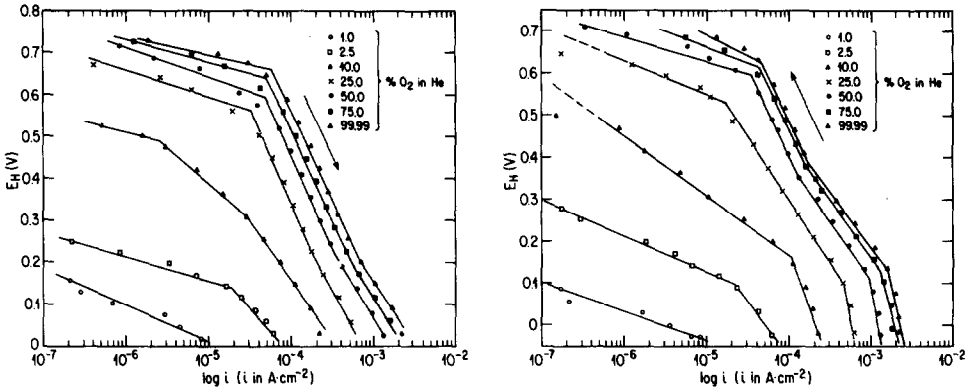

Fig. 7. Potentiostatic potential–log [current] relationships for the o.d.r. on Co–WC in 1M KOH solutions, at various concentrations of O_2 in He. The temperature is 25 °C and the rotation rate of the disk is 2000 r.p.m. The data pertain to the descending direction of potentials (see the arrow).

Fig. 8. As in Fig. 7 but now in the ascending direction of electrode potentials, as indicated by the arrow.

this is not at all unexpected at these potentials at which the reduction of oxygen is proceeding at high rates, so that the reaction tends to be limited by a diffusion process. Similar ΔH^* values are also obtained at the intermediate values of the o.d.r. overpotential, *i.e.*, 0.3 V (Figs. 5 and 6); at the lower overpotentials, the ΔH^* values become higher and approach those diagnostic of an activation-controlled reaction (Figs. 5 and 6).

(iii) The effect of oxygen concentration on the rate of reduction

The rate of electro-reduction of oxygen has been examined as a function of the concentration of oxygen, both in the descending (Fig. 7) and the ascending (Fig. 8) direction of electrode potentials; the separation of these data into two graphs is dictated, again, by the need to avoid an unmanageable clutter. We have tried to constrain straight lines through various regions of high slopes.

The rate, at a given electrode potential, increases with increasing concentration of oxygen, as expected from theory. At the highest overpotential studied, the order of reaction with respect to oxygen is near unity, *i.e.*,

$$\left(\frac{\partial \log i}{\partial \log O_2}\right)_{N,\,T,\,pH\ldots} \simeq 1.$$

This result is presented in Fig. 9; also included are the same data for the o.d.r. on WC.

(iv) The effect of pH on the reaction rate

The rate of oxygen reduction on Co–WC has also been investigated in solutions of different pH values but constant ionic strengths (Fig. 10). It

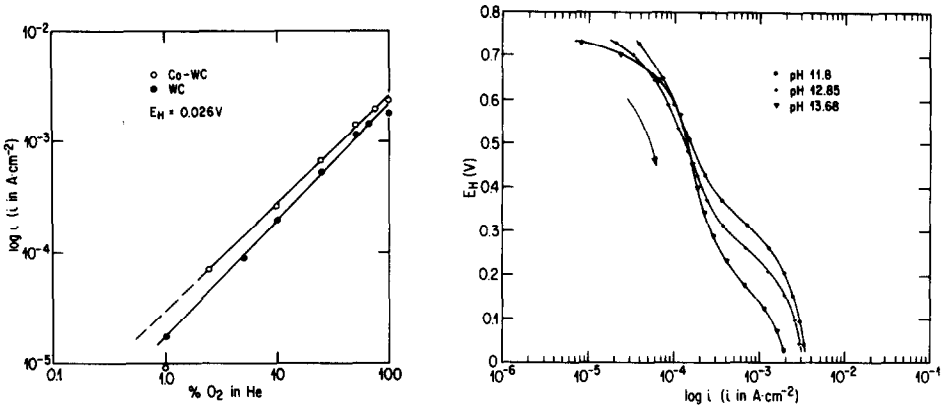

Fig. 9. A plot of the reaction rate (*i.e.*, log [current density]) at the highest overpotential for the o.d.r. studied in the present work (*i.e.*, 0.026 V) against the concentration of oxygen; the data refer to both the descending and the ascending direction of potentials (*i.e.*, Figs. 7 and 8) since the same rate is observed at the overpotentials (*i.e.*, 0.026 V *vs.* RHE) shown. The same data for the WC have also been added to the plot. The reaction order w.r.t. to O_2 is around unity, both for Co–WC and WC (see Table 1).

Fig. 10. Potential–log [current] relationships for the o.d.r. on Co–WC in 1M KOH solutions at various pH values in solutions of constant ionic strengths. The data are for 25 °C and a disk rotation of 2000 r.p.m.; descending direction of potentials (see the arrow). Very similar data are obtained on Co–WC for the ascending direction of potentials. Nearly identical pH effects are also observed on WC (see Table 1).

appears that at higher overpotentials, the rate exhibits a slight negative reaction order with respect to the hydroxyl ions (Fig. 10); similar results are also obtained in the ascending direction of electrode potentials.

(v) The comparison of results on WC and Co–WC

Most of the experimental results on the electro-reduction of oxygen are very similar (Table 1) on WC and Co–WC (see also Fig. 9); there are some notable differences, however. For example, the temperature-dependence of rate (Fig. 11) on WC is much less marked than that on Co–WC; this is also reflected in the very low values of the apparent heats of activation (Fig. 12) derived from the data in Fig. 11. On the other hand, the reaction order with respect to oxygen is near unity (Fig. 9), as for the case of Co–WC.

Discussion

In order to elucidate fully the mechanism of o.d.r., it is desirable to conduct kinetic studies on a disk-ring electrode. In the present case, it was considered necessary to avoid the usual platinum ring since it can "contaminate" the solution with platinum ions, especially at the anodic potentials to which the concentric ring must be subjected [2]. This difficulty is particu-

TABLE 1

Electro-reduction of oxygen on Co–WC and WC electrodes

Parameter	Value for Co–WC	Value for WC
(1) Tafel slopes	~ RT/F at low η and low temperature values; ~ $6(RT/F)$ at higher η values	Tafel region difficult to define at low η at any temperature; ~ $6(RT/F)$ at higher η values
(2) Temperature-dependence of rate, *i.e.*, ΔH^*	ΔH^* values approach 5 kcal mol^{-1} at high η; ΔH^* values near ~ 10 kcal $mole^{-1}$ at low η	ΔH^* less than ~ 5 kcal $mole^{-1}$ at all η values
(3) Rotation-dependence of current	Some rotation-dependence at high η	Some rotation-dependence at high η
(4) Reaction order w.r.t. O_2	~ unity	~ unity
(5) pH-dependence of rate	~ slight negative reaction order w.r.t. OH^-	~ slight negative reaction order w.r.t. OH^-

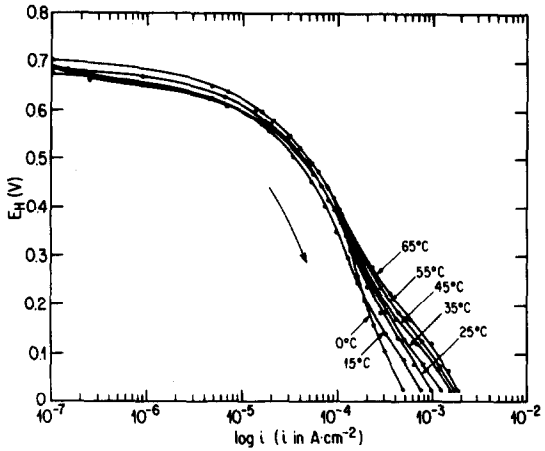

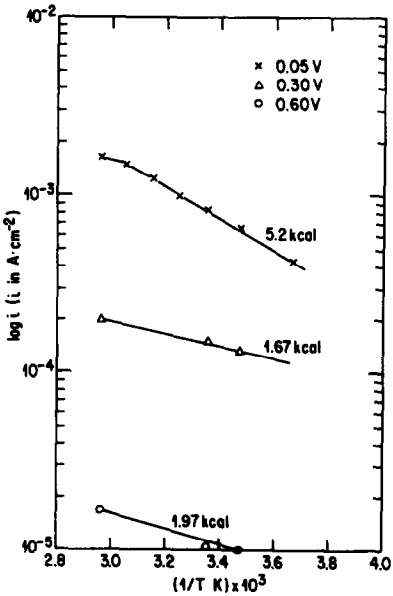

Fig. 11. Potentiostatic potential–log [current] relationship for the o.d.r. on WC in 1M KOH at various temperatures in the descending direction of electrode potentials (*cf.* Fig. 3 for Co–WC); the electrode rotation rate is 2000 r.p.m.

Fig. 12. The plots for the apparent heat of activation, ΔH^*, values on WC (*cf.* Fig. 5 for Co–WC); the primary data are taken from Fig. 11.

larly pronounced when one is examining the kinetics of o.d.r. at a relatively non-catalytic, non-noble electrode, as in the present case.

For o.d.r., it is observed that, in general, at low current densities oxygen is reduced to hydrogen peroxide [3]. At higher current densities, oxygen is initially reduced to hydrogen peroxide, which is subsequently reduced to hydroxyl ions in the alkaline solutions. This type of reduction path for the oxygen is also indicated in the present results where a slight dependence on the rotation rate is observed at the higher current densities only (Figs. 1 and 2).

From Table 1, it is clear that, in general, very high Tafel slopes ($\approx 6RT/F$) and low apparent heats of activation are the kinetic characteristics for the o.d.r. in the present case, both on Co–WC and WC. Thus the rather low dependence of the reaction rate both on the electrode potential and the temperature suggests that the rate-determining step (r.d.s.) does not perhaps involve a charge transfer but is probably a chemical step. Further, this chemical step cannot be diffusion controlled since the dependence on electrode rotation is slight and occurs only at high current densities, most likely owing to the reduction of the reaction intermediate H_2O_2 to hydroxyl ions. These data would thus suggest a mechanism such as the following [4]:

$$2S + O_2 + H_2O \rightarrow S - HO_2 + S - OH \quad (1)$$

$$S - HO_2 + e \rightarrow S + HO_2^- \quad (2)$$

$$S - OH + e \rightarrow S + OH^- \quad (3)$$

$$S - OH + S - OH \rightarrow 2S + H_2O_2. \quad (4)$$

Here S denotes a substrate site, *i.e.*, a site on the electrode. A chemical step such as (1) or (4) would be the probable r.d.s. The peroxide formed can, of course, undergo a further electrochemical reduction to give hydroxyl ions, probably at higher current densities. The experimental value of the reaction order with respect to oxygen (Table 1) would suggest, rather unambiguously, reaction (1) as the r.d.s., both on Co–WC and WC. Finally, this rate-determining step would predict no pH-dependence, again consistent with the rather negligible dependence on pH observed here (Fig. 10). The slight negative reaction order at higher pH values perhaps arises from enhanced specific adsorption of OH^- in more alkaline solutions [5].

It is pertinent to the present work to illustrate certain other features of the experimental data. In the introductory comments in the section on "Results", it has been stated that the anodic dissolution currents noted in the absence of O_2 disappear when O_2 is bubbled through the solutions. This is confirmed, in a complementary way, by data in Fig. 13 depicting the "rest potentials" (*i.e.*, the open-circuit mixed potentials) of the oxygen. The electrode potentials are less noble at low concentrations of oxygen but tend to approach a limiting value (*ca.* 0.8 V) at higher concentrations of O_2; thus the stable condition of the electrodes at high O_2 concentrations is also indicated by the stable, limiting rest potentials. Since these open-circuit potentials are mixed potentials, no mechanistic significance can be attached to them.

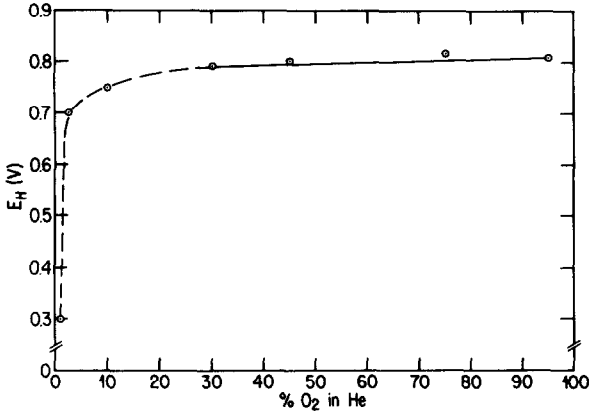

Fig. 13. A plot of open-circuit "rest potentials" of Co–WC in 1M KOH at various concentrations of O_2.

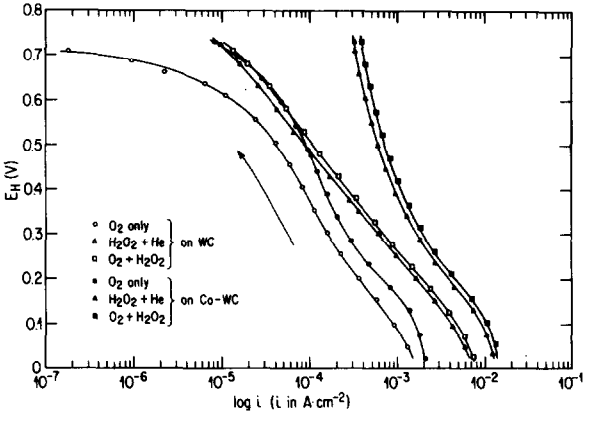

Fig. 14. A point-by-point potentiostatic potential–log [current] relationship in 1M KOH on WC and Co–WC; the concentration of O_2 is 100% and of H_2O_2 is 0.1M. The experiments were carried out on a rotating disk electrode at 2000 r.p.m. and at 23 °C; the data shown refer to the ascending directions of potentials, as indicated by the arrow.

In the context of the present discussion, it is also pertinent to examine the activity of the electrodes for the reduction of H_2O_2. This has been done in Fig. 14 which compares the activity for the reduction of O_2 of both WC and Co–WC with that for H_2O_2 reduction. The electro-reduction of H_2O_2 exhibits much higher rates than the O_2 reduction, both on WC and Co–WC. This is in agreement with previous work from these laboratories [6, 7] in which a variety of bronzes and oxides showed similar characteristics. Also, the presence of Co enhances the activity of WC for all these reductions, *i.e.*, O_2, H_2O_2, and $O_2 + H_2O_2$; this result would thus be consistent, in a general way, with the previous observation [1] in which the presence of Co imparted a considerable activity to WC for the anodic oxidation of hydrazine.

Conclusion

The electro-activity of WC and Co–WC for the reduction of O_2 and H_2O_2 is very similar to that observed on bronzes and oxides. In alkaline solutions the electrodes are stable in the potential region *ca.* 0 - 0.7 V (RHE), after the initial "conditioning" current–potential curve. These electrodes show some catalytic activity for the O_2 reduction; their activity towards the reduction of H_2O_2 is much more pronounced, however.

Acknowledgment

Thanks are due to Mr Alain Joly of the Direction Matériaux - Recherche et Essais, IREQ, for the X-ray fluorescence analyses of the electrode surfaces.

References

1 A. K. Vijh, G. Bélanger and R. Jacques, *J. Power Sources, 6* (1981) 229.
2 A. K. Vijh and G. Bélanger, *Corros. Sci., 16* (1976) 869.
3 M. A. Genshaw, A. Damjanovic and J. O'M. Bockris, *J. Electroanal. Chem., 15* (1967) 163, 173.
4 A. Damjanovic, in J. O'M. Bockris and B. E. Conway (eds.), *Modern Aspects of Electrochemistry*, Vol. 5, Plenum Press, New York, 1969, p. 369.
5 Ch. Fabjan, M. R. Kazemi and A. Neckel, *Ber. Bunsenges. Phys. Chem., 84* (1980) 1026.
6 J.-P. Randin, *J. Electroanal. Chem., 51* (1974) 471.
7 J.-P. Randin, *J. Electrochem. Soc., 121* (1974) 1029.